Thermorudis pharmacophila WKT50.2^T sp. nov., a novel isolate of class *Thermomicrobia* isolated from geothermal soil, and emended descriptions of *Thermomicrobium roseum*, *Thermomicrobium carboxidum*, *Thermorudis peleae* and *Sphaerobacter thermophilus*.

Karen M. Houghton[1,2], Xochitl C. Morgan[3], Kirill Lagutin[4], Andrew D. MacKenzie[4], Mikhail Vyssotskii[4], Kevin A. Mitchell[4], Ian R. McDonald[2], Hugh W. Morgan[2], Jean F. Power[1], John W. Moreau[5], Eric Hanssen[5] and Matthew B. Stott[1]

[1]GNS Science, Extremophiles Research Group, Private Bag 2000, Taupō, 3352, New Zealand

[2]School of Science, University of Waikato, Private Bag 3105, Hamilton 3240, New Zealand

[3]Department of Biostatistics, Harvard T. H. Chan School of Public Health, 655 Huntington Ave., Boston MA 02115, USA

[4]Callaghan Innovation, PO Box 31310, Lower Hutt 5040, New Zealand

[5]University of Melbourne, 30 Flemington Road, Victoria 3010, Australia

Running title: *Thermorudis pharmacophila*

New Taxa: Other Bacteria

GenBank/EMBL/DDBJ accession number of the 16S rRNA gene sequence of *Thermorudis pharmacophila* is HE794997.

Abbreviations: CMC, carboxymethylcellulose; TEM, transmission electron microscopy; TLC, thin layer chromatography.

ABSTRACT

An aerobic, thermophilic and cellulolytic bacterium, designated strain WKT50.2^T, was isolated from geothermal soil at Waikite, New Zealand. Strain WKT50.2^T grew at 53-76 °C, and at pH 5.9-8.2. The DNA G+C content was 58.4 mol%. The major fatty acids were 12-methyl $C_{18:0}$ and $C_{18:0}$. Polar lipids were all linked to long chain 1,2-diols, and comprised of 2-acylalkyldiol-1-*O*-phosphoinositol (diolPI), 2-acylalkyldiol-1-*O*-phospho-acylmannoside (diolP-acylMan), 2-acylalkyldiol-1-*O*-phosphoinositol acylmannoside (diolPI-acylMan) and 2-acylalkyldiol-1-*O*-phosphoinositol mannoside (diolPI-Man). Strain WKT50.2^T was utilised a range of cellulosic substrates, alcohols and organic acids for growth, but was unable to utilise monosaccharides. Robust growth of WKT50.2^T was observed on protein derivatives. WKT50.2^T was sensitive to ampicillin, chloramphenicol, kanamycin, neomycin, polymyxin B, streptomycin and vancomycin. Metronidazole, lasalocid A and trimethoprim stimulated growth. Phylogenetic analysis of 16S rRNA gene sequences showed that WKT50.2^T belonged to class *Thermomicrobia* within the phylum *Chloroflexi*, and was most closely related to *Thermorudis peleae* KI4^T (99.6 %). DNA-DNA hybridization of WKT50.2^T and *T. peleae* KI4^T was 18.0 %. Physiological and biochemical tests confirmed phenotypic and genotypic differentiation of strain WKT50.2^T from *T. peleae* KI4^T and other *Thermomicrobia*. On the basis of its phylogenetic position and phenotypic characteristics, we propose that strain WKT50.2^T represents a novel species for which the name *Thermorudis pharmacophila* sp. nov. is proposed, with the type strain WKT50.2^T (=DSM 26011^T =ICMP 20042^T).

Emended descriptions of the strains *T. roseum, T. carboxidum, T. peleae* and *S. thermophilus* are also proposed and include the description of a novel respiratory quinone, MK-8 2,3-epoxide (23 %) in *T. roseum.*

Members of the class *Thermomicrobia* are broadly distributed across a wide range of both aquatic and terrestrial habitats including geothermally-heated soils, sediments and hot springs (Costa *et al.*, 2009; Engel *et al.*, 2013), mesophilic soils (Joynt *et al.*, 2006; Lesaulnier *et al.*, 2008) and rock (De la Torre *et al.*, 2003). In addition, they have been detected in compost (Partanen *et al.*, 2010; Gladden *et al.*, 2011), sewage sludge (Demharter *et al.*, 1989) and on human skin (Grice *et al.*, 2009). *Thermomicrobia* is comprised of five characterised isolates with validly-published names: *Thermomicrobium roseum* (Jackson *et al.*, 1973) isolated from a hot spring, *Sphaerobacter thermophilus* (Hugenholtz & Stackebrandt, 2004) isolated from sewage sludge, *Nitrolancea hollandicus* (Sorokin *et al.*, 2014) isolated from a nitrifying bioreactor, and *Thermorudis peleae* and *Thermomicrobium carboxidum* (King & King, 2014b) isolated from a volcanic soil biofilm. Although the genomes of both *T. roseum* and *S. thermophilus* are available (Wu *et al.*, 2009; Pati *et al.*, 2010), they have only been partially characterised. It has further been suggested that *Candidatus* "Thermobaculum terrenum" (Botero *et al.*, 2004) may also be incorporated into the *Thermomicrobia*, although its phylogenetic position is uncertain and remains contentious (Kunisawa, 2011; Gupta *et al.*, 2013). All *Thermomicrobia* strains are neutrophilic, either thermotolerant or thermophilic, and have a broad chemoorganotrophic substrate specificity.

Here we describe the phenotypic and phylogenetic characteristics of a novel *Thermomicrobia* strain, WKT50.2^T, which was isolated from geothermally-heated soil in New Zealand. We propose that it represents a novel species within the genus *Thermorudis*. In addition, we performed supplementary characterisation of *T. roseum* (Jackson *et al.*, 1973), *T. carboxidum* and *T. peleae* (King & King, 2014b), and *S. thermophilus* (Demharter *et al.*, 1989) and propose the emendation of their formal descriptions.

Strain WKT50.2^T was isolated from geothermally-heated soil at Waikite, New Zealand. Soil gas fluxes at Waikite are low and are composed principally of CO_2 (>95 mol %) with minor concentrations of NH_3 and CH_4 (Giggenbach *et al.*, 1994). The soil was sampled from a pink-coloured soil profile directly above the hot spring. The soil sample had a pH of 4.5 (25 °C) and an *in situ* temperature of 64.8 °C. Soil crumbs were spread on AOM1 plates (Stott *et al.*, 2008) and incubated at 60 °C in an aerobic atmosphere. Individual bacterial colonies were picked and purified with the streak-plate method until an axenic culture was obtained (Stott *et al.*, 2008). Unless otherwise stated, all physiological and metabolic characteristics were determined by growing WKT50.2^T at 65 °C in liquid CPS medium (Supplementary Information), and all materials and methodologies for phenotypic characterisation have been listed in the Supplementary Information.

Genomic DNA was isolated from strain WKT50.2^T using a NucleoSpin Tissue kit (Macherey Nagel, Germany) according to the manufacturer's instructions. The 16S rRNA gene was amplified using the

universal bacterial primers 9F and 1492R (Weisburg *et al.*, 1991). The near-complete 16S rRNA gene sequence was 1357 bp (HE794997), and was manually checked for quality. Closely-related strains to WKT50.2^T were determined by subjecting the 16S rRNA gene sequence to blastN discontiguous megablast search (Altschul *et al.*, 1997). The 16S rRNA gene sequences from WKT50.2^T and closely-related strains and phylotypes were aligned (all retrieved sequences were > 1212 bp in length), and phylogenetic distances were calculated using the Jukes-Cantor correction within the ARB software environment - SILVA SSU NR (non-redundant) Release 119 database (Jukes & Cantor, 1969; Ludwig *et al.*, 2004). WKT50.2^T was most closely related to *T. peleae* KI4^T (99.6 %)*, T. carboxidum* KI3^T (91.6 %) and *T. roseum* DSM 5159^T (91.2 %). A phylogenetic tree (Fig. 1) was constructed using MrBayes, which uses a Bayesian inference model to calculate phylogeny (Ronquist *et al.*, 2012). The phylogenetic tree in Figure 1 was calculated using a 0.25 burn, and Markov Chain Monte Carlo (MCMC) estimation of 2,000,000 cycles, four chains (temperature parameter of 0.5) and a sampling frequency of 500. The phylogenetic placement of strain WKT50.2^T shows that it groups within class *Thermomicrobia* and is a member of the genus *Thermorudis* (Fig. 1).

Strain WKT50.2^T formed pale pink, convex and entire colonies of 2-3 mm diameter after two days of incubation on CPS medium at 70 °C. Gram staining was negative. No cell lysis was observed when cells were treated with a 3 % (v/v) solution of KOH (Halebian *et al.*, 1981). Neither motility nor spore formation were observed under any growth conditions. WKT50.2^T cells had a characteristic dumb-bell, or short rod morphology (Fig. 2). As the cultures aged, pairs or chains of cells were frequently observed. Cells were between 2.1 and 2.8 µm long, and 0.9 to 1.1 µm wide (Fig. 2a). Cryo-TEM of WKT50.2^T cells showed a classical Gram-negative structure of a cytoplasmic membrane, a peptidoglycan layer, outer membrane, and putative thin proteinaceous and/or polysaccharide-rich S-layer (Fig. 2b). The widths of the two cited lipid membranes are approximately 6 nm (data not shown), which is consistent with a typical membrane thickness of 4-7 nm. The peptidoglycan composition (Schumann, 2011) and cell wall sugars (Staneck & Roberts, 1974) of WKT50.2^T were analysed by the Identification Service of the Deutsche Sammlung für Mikroorganismen und Zellkulturen (DSMZ), Braunsweig, Germany. The analysis found substantial amounts of protein present in the cell membrane, which could not be fully removed from the cell hydrolysate and therefore prevented full analysis of the peptidoglycan content. No diaminopimelic acid (DAP) was detected in WKT50.2^T cell walls, but ornithine, L-alanine and D-glutamic acid were identified and are normally associated Gram-positive type cell membranes (Schleifer & Kandler, 1972). The same amino acids were detected in the cell wall of *N. hollandicus* (Sorokin *et al.*, 2014). The cell envelopes of *T. roseum* and *S. thermophilus* were also composed largely of protein, and only minor concentrations of peptidoglycan could be detected (Merkel *et al.*, 1980) (Demharter *et al.*, 1989) The

cell wall sugars of WKT50.2^T were determined by TLC and contained xylose, mannose, glucose, galactose, rhamnose and ribose. These sugars are not routinely reported in bacterial cell walls, but with the exception of ribose, they reflect the composition of the large polysaccharide complex bound to the peptidoglycan observed in the monoderm *Chloroflexus aurantiacus* (Jürgens *et al.*, 1987; Meissner *et al.*, 1988). These data suggest that the cell envelope of WKT50.2^T (Fig. 2b) includes substantial polysaccharide and protein components.

Fatty acid methyl esters (FAMEs) were prepared and analysed as previously described (Lagutin *et al.*, 2014). The fatty acid composition of WKT50.2^T is presented in Table S1. The cell membrane of WKT50.2^T was primarily composed of the fatty acids 12-methyl $C_{18:0}$ (54.0 %) and $C_{18:0}$ (30.6 %). Polar lipids were analysed using TLC and phospholipids were quantified by ^{31}P-NMR (MacKenzie *et al.*, 2009) (Supplementary Information). TLC analysis of polar lipids indicated seven glycolipids and four unknown phospholipids (Fig. S1). Phospholipids comprised 25.2 % of the total lipids and included four unusual 1,2-diol-linked lipids (Lagutin *et al.*, 2014); 2-acylalkyldiol-1-*O*-phosphoinositol (diolPI) (64.0 mol%), 2-acylalkyldiol-1-*O*-phospho-acylmannoside (diolP-acylMan) (17.9 mol%), 2-acylalkyldiol-1-*O*-phosphoinositol acylmannoside (diolPI-acylMan) (11.5 mol%) and 2-acylalkyldiol-1-*O*-phosphoinositol mannoside (diolPI-Man) (6.7 mol%) (Table S2, Figs. S2 and S3). Diol-linked lipids were previously reported in *T. roseum* (Pond *et al.*, 1986) and *N. hollandicus* (Sorokin *et al.*, 2012) but were not fully characterised.

DNA base composition and DNA-DNA hybridisation were determined by the Identification Service of the DSMZ. The %G+C base content was determined by disrupting cells via French pressure cell and purifying the DNA extract using a hydroxyapatite column (Cashion *et al.*, 1977). The DNA was hydrolysed with P1 nuclease and dephosphorylated with bovine alkaline phosphatase and then quantified using HPLC (Mesbah *et al.*, 1989). The DNA base composition was 58.4 mol% G+C. DNA-DNA hybridisation between WKT50.2^T and *T. peleae* was performed as previously described (Ziemke *et al.*, 1998). Strain WKT50.2^T and *T. peleae* KI4^T exhibited a mean DNA-DNA similarity of 18.0 %, which is below the recommended threshold value of 70 % for bacterial species delineation (Wayne *et al.*, 1987). The extraction and determination of the respiratory quinones was undertaken using a modified LCMS method (Supplementary Information) described by Nishijima and colleagues (Nishijima *et al*., 1997) and was determined as MK-8 (95.3 %) and MK-9 (4.7%).

Strain WKT50.2^T was unable to grow anaerobically using sulphur, sulphate or nitrate as terminal electron acceptors (Supplementary Information). It had a growth range between 53–76 °C (optimum 68-73 °C), and the pH range for growth was pH 5.9-8.2 (optimum pH 6.8-7.0). No growth was observed at or below pH 5.5, or at or above pH 8.9. Growth was observed with 0-1 % (w/v) NaCl, but

optimum growth occurred in the absence of NaCl. All substrate utilization experiments were conducted in triplicate, with shaking incubation at 125 r.p.m. at 68 °C, using Castenholz salts solution (Supplementary Information) with 50 % (v/v) air headspace. Table S3 contains a list of substrates tested (0.2 % w/v unless otherwise stated). WKT50.2^T grew chemoorganotrophically using some di- and trisaccharide substrates, but no growth was observed when using monosaccharides or sugar derivatives as sole energy sources. WKT50.2^T was able to hydrolyse soluble starch (Sigma-Aldrich), crystalline cellulose (Avicel™, Sigma-Aldrich) and sodium CMC (Hercules). Organic acids, with the exception of sodium citrate, were used as sole carbon sources. Growth was also observed in media containing peptone (Oxoid), Bacto™ tryptone (BD), Casamino acids (Difco) or BBL™ yeast extract (BD), as well as in standard complex media such as R2A and nutrient broth. Ethanol and methanol were utilised as sole carbon sources, but not 1-propanol or 2-propanol (all 0.05 % v/v). Oxidation of carbon monoxide was tested as previously described (Hardy & King, 2001) but was not observed. No homologs of the gene of the large subunit of carbon monoxide dehydrogenase (*coxL*) were found using PCR primers (Table S4) based on the gene sequences from *T. roseum* and *S. thermophilus,* or through analysis of the draft genome of WKT50.2^T. The preferred nitrogen source was determined by providing different nitrogen sources in otherwise nitrogen-free Castenholz salts solution with sucrose as a carbon and energy source (Supplementary Information). Nitrogen sources tested were N_2, KNO_3, KNO_2, $(NH_4)_2SO_4$, yeast extract, urea, alanine, and serine. Strain WKT50.2^T was able to use nitrate, ammonia and alanine as sole nitrogen sources.

Antibiotic sensitivity was assessed by growing strain WKT50.2^T on Castenholz salts solution with 5 g l^{-1} peptone and 2.5 g l^{-1} sucrose, with either 3 or 30 µg ml^{-1} antibiotic. No growth was observed with the addition of 3 µg ml^{-1} ampicillin, which possibly supports a peptidoglycan assembly structure in the cell, chloramphenicol, kanamycin, neomycin, polymyxin B, streptomycin or vancomycin. The addition of 3 µg ml^{-1} lasalocid A, or 3 or 30 µg ml^{-1} metronidazole or trimethoprim resulted in a higher OD_{600} as well as a faster growth rate than the control with no antibiotic added (Table S5). Further experiments showed a dosage-dependent increase in growth of WKT50.2^T following the addition of up to 150 µg ml^{-1} metronidazole or trimethoprim (data not shown). Neither metronidazole, lasalocid A nor trimethoprim were able to support growth as sole carbon or nitrogen sources.

Strain WKT50.2^T demonstrated negative reactions for both catalase and oxidase. Other enzyme activities were assessed using the API ZYM kit (bioMérieux), prepared according to the manufacturers' instructions. Esterase (C4), esterase lipase (C8), lipase (C14), leucine arylamidase, valine arylamidase, and trypsin activities were observed (Table S6).

In addition to the characterisation of WKT50.2^T we undertook further chemotaxonomic or phenotypic analysis of the type strains of *T. roseum* (DSM 5159^T), *T. peleae* (DSM 27169^T), *T. carboxidum* (DSM 27067^T) and *S. thermophilu*s (DSM 20745^T). The materials and methods used for this characterisation are described in full in the Supplementary Information, but where possible, reflect the methodologies used for the WKT50.2^T characterisation. The temperature and pH ranges and optima for growth, substrate utilisation (Table S3), preferred nitrogen sources and salinity tolerance were determined for *T. roseum* and *S. thermophilus*. The growth responses to metronidazole, lasalocid A and trimethoprim were also determined (Table S5). Full results are found in the emended species descriptions for these type species. The respiratory quinone content of *T. roseum* was determined by LC-MS (Supplementary Information) and was composed of primarily MK-8 (74 %) along with low levels of MK-9 (3 %). A third peak (23 %) observed in the LC-MS chromatograph (Fig. S4) corresponded to a novel quinone. We analysed this unknown peak (Supplementary Information) and determined that it is an MK-8 epoxide with the epoxy structure at the 2,3 position (see Supplementary Information and Figs. S5-S6). ^{31}P-NMR analysis of the *S. thermophilus* lipid extract identified the same four phospholipids as found in WKT50.2^T; diolPI (41.3 mol%), diolP-acylMan (17.0 mol%), diolPI-acylMan (8.4 mol%) and diolPI-Man (33.3 mol%) and comprised 53.5 % of total lipid extract (Lagutin *et al.*, 2014). The FAME content of *S. thermophilus* was dominated by 12-methyl $C_{18:0}$ (63.2 %) and $C_{18:0}$ (17.1 %) and reflects the FA profile of WKT50.2^T (54.0 % and 30.6 % respectively). The unusual fatty acid 12-methyl $C_{18:0}$ was previously determined to be the major fatty acid in *T. roseum* (68 %) (Pond *et al.*, 1986) and *N. hollandicus* (Sorokin *et al.*, 2012), and was found at low levels (1.6 – 7.6 %) in *Thermogemmatispora* strain T81 (Vyssotski *et al.*, 2012). Outside the phylum *Chloroflexi*, 12-methyl $C_{18:0}$ fatty acid has only been detected in low concentrations (< 5 %) in *Rubrobacter xylanophilus* (Carretto *et al.*, 1996) and two strains of *Rubrobacter taiwanensis* (Chen *et al.*, 2004). This fatty acid has not been found in the closely-related species *R. radiotolerans* (Suzuki *et al.*, 1988), and thus could be considered as a useful taxonomic marker for the class *Thermomicrobia.*

Despite the classical diderm-type cell envelope observed in Cryo-TEM imaging of WKT50.2^T (Fig. 2b) and a negative Gram stain reaction, a number of chemotaxonomic observations reported here were more consistent with the characteristic monoderm envelope structure normally associated with the phylum *Chloroflexi*. The lack of detectible concentrations of DAP and presence of ornithine, L-alanine and D-glutamic acid in the cell wall lysate, a negative KOH reaction and susceptibility to vancomycin and ampicillin are all characteristic of Gram-positive, monoderm-type cell envelope structures. Indeed, previous cell envelope classifications of *Chloroflexi* strains have been inconsistently reported due to variable Gram-staining results for *Chloroflexus aurantiacus*, *Herpetosiphon* and *Roseflexi* spp.,

despite the prevailing *Chloroflexi* monoderm consensus (Sutcliffe, 2010 and references therein). Recent publications reviewing the cell envelopes of *Chloroflexi* have argued that all *Chloroflexi* genomes (including *T. roseum*, *T. terrenum* and *S. thermophilus*) lack crucial genes required for LPS production and transport, and transporters specific to cell walls (Sutcliffe, 2010; Sutcliffe, 2011). We have reviewed the draft genome of WKT50.2^T (not shown) and were also unable to find evidence of crucial gene homologs required for the function and synthesis of diderm-type cells (Supplementary information), nor secretory systems linked with the outer membrane. Based upon the lack of genomic evidence for a diderm-type cell envelope and chemotaxonomic observations consistent with monoderms, we conclude that WKT50.2^T has an atypical monoderm cell envelope rich in proteinaceous and polysaccharide materials. Previous reports cite multi-layered outer membranes structures for *Thermogemmatispora onikobensis* and *Thermogemmatispora foliorum* (Yabe *et al.*, 2011), *C. aurantiacus* (Hanada and Pearson, 2006) and other *Chloroflexi* spp. (Jürgens *et al.*, 1987), although the composition and purpose of these structures have yet to be investigated. We therefore caution that a focussed investigation of cell envelopes of *Chloroflexi* isolates that includes electron microscopy, chemotaxonomic and genomic analyses is warranted and should be undertaken in the future to provide clarity in cell envelope classification across this phylum.

Strain WKT50.2^T could be differentiated from other *Thermomicrobia* members on the basis of both phenotypic and chemotaxonomic features, including differences in temperature and pH range, substrate utilisation, oxidase and catalase reactions, Gram-staining and %G+C content of genomic DNA (Table 1). It placed phylogenetically within the class *Thermomicrobia* and had the greatest 16S rRNA gene sequence similarity with *T. peleae* (99.6 %), *T. carboxidum* (91.6 %) and *T. roseum* (91.2 %). DNA–DNA hybridization between *T. peleae* and WKT50.2^T was less than the 70 % DNA-DNA similarity species-level threshold (Wayne *et al.*, 1987) confirming that WKT50.2^T is a novel species. In addition, WKT50.2^T was able to utilise several substrates which *T. peleae* could not, including sucrose, glycerol, ethanol, methanol and organic acids such as acetate, pyruvate and succinate. WKT50.2^T was unable to utilise any monosaccharides tested (Table 1). In contrast, *S. thermophilus* was able to utilize fructose as a monosaccharidic energy source, and *T. roseum* exhibited growth using all monosaccharides tested (Table 1). The growth of WKT50.2^T was promoted by the cultivation in the presence of lasalocid A, metronidazole and trimethoprim whereas *T. peleae* and *T. carboxidum* only exhibited resistance to metronidazole and trimethoprim and not promoted growth. In contrast to *T. roseum, S. thermophilus*, and *T. carboxidum,* WKT50.2^T was unable to use carbon monoxide as an energy source or oxidise it constitutively. It is interesting to note that this inability is also shared with *T. peleae* (King & King, 2014b), and it therefore is tempting to infer that this observation could be used as a diagnostic tool to differentiate *Thermorudis* from *Thermomicrobium*

spp. However, we believe that this observation is likely coincidental particularly as the ability to oxidise CO by other *Chloroflexi* such as by *Thermogemmatispora* spp. (King & King, 2014a) appears to be independent of 16S rRNA gene phylogeny. These findings indicate that strain WKT50.2^T is phylogenetically and physiologically distinctive from other species within the class *Thermomicrobia* and we therefore propose that it represents a novel species within the genus *Thermorudis, T. pharmacophila* WKT50.2^T. The descriptions of the species *T. roseum*, and *S. thermophilus* are emended on the basis of new fatty acids, polar lipids, antibiotic resistance, quinones and substrate utilisation data. Emended descriptions of *T. carboxidum* and *T. rudis* are also provided.

Description of *Thermorudis pharmacophila* sp. nov.

Thermorudis pharmacophila (phar.ma.co'phi.la. Gr. neut. n. *pharmakon* poison; N.L. adj. *philus* -a -um (from Gr. adj. *philos* -ê-on) loving; N.L. fem. adj. *pharmacophila*, poison-loving).

Has the following characteristics in addition to those given in the genus description (King & King, 2014b). Cells are rods approx. 0.9 - 1.1 µm in diameter and 2.1 - 2.8 µm in length. Exhibits an oxidative, heterotrophic metabolism. No growth observed on monosaccharides. Sucrose, trehalose and raffinose act as sole carbon sources; lactose, maltose and cellobiose do not. Avicel™, CMC, starch, and xylan are hydrolysed, but chitin, dextrin, gellan gum, galactomannan, glucomannan, pectin and xanthan are not. Cells also grow on Whatman™ filter paper, glycerol, sorbitol and 0.05 % (v/v) methanol or ethanol. Sodium acetate, formate, fumarate, lactate, pyruvate and succinate act as sole carbon sources; sodium citrate, mannitol, galacturonic acid and 0.05% 1–propanol or 2-propanol do not. Cells grow readily on yeast extract, peptone, tryptone and Casamino acids. Growth inhibited by ampicillin, chloramphenicol, kanamycin, neomycin, polymyxin B, streptomycin and vancomycin. Lasalocid A, metronidazole and trimethoprim stimulate growth. Ammonium ion, nitrate ion or alanine can act as sole nitrogen sources. Optimal growth at 68-73 °C (range: 53-76 °C) and pH 6.8–7.0 (range: 5.9–8.2). NaCl tolerance up to 1 % (w/v). Growth on solid gellan-based medium produces pink opaque colonies with circular and entire edges. G+C content of strain WKT50.2^T is 58.4 mol% and the principal quinone detected is MK-8 with minor concentrations of MK-9. The major fatty acids are 12-methyl $C_{18:0}$ and $C_{18:0}$, with minor amounts of $C_{20:0}$, $C_{16:0}$, 10-methyl $C_{16:0}$ and $C_{14:0}$. Polar lipids are diol-linked and include diolPI, diolP-acylMan, diolPI-acylMan and diolPI-Man.

The type strain, WKT50.2^T (=DSM 26011^T =ICMP 20042^T) was isolated from geothermally-heated soils at Waikite, New Zealand.

Emended description of *Thermomicrobium roseum* Jackson *et al.* 1973

The description is as given by Jackson *et al.* (1973) with the following amendments.

Growth occurs on simple sugars; D-xylose, D-galactose, D-mannose, D-fructose, D-cellobiose, D-maltose, sucrose, D-trehalose and D-raffinose. Dextrin, Phytagel™, starch, xylan and xanthan act as sole carbon sources, but Avicel™ and CMC do not. Grows on short-chain alcohols including methanol, ethanol, 1-propanol, 2-propanol and mannitol, but not sorbitol. Cells also grow on glycerol and sodium acetate, formate, fumarate, lactate, pyruvate and succinate but not citrate. Peptone, tryptone and Casamino acids act as sole carbon sources. Ammonium ion, nitrate ion or yeast extract can act as sole nitrogen sources. Growth is stimulated by metronidazole and trimethoprim. The predominant quinones are MK-8, MK-8 2,3-epoxide and MK-9, and the major fatty acid is 12-methyl $C_{18:0}$. Fatty acids are linked to diols. Optimal growth at 65-70 °C (range: 52-77 °C) and pH 8.0-8.4 (range: 6.0-9.4). NaCl tolerance up to 1.5 % (w/v). Cells possess cell envelopes composed largely of protein with only small amounts of peptidoglycan, and ornithine is present.

The type strain, *Thermomicrobium roseum*^{T} (= DSM 5159 = ATCC 27502) was isolated from a geothermal hot spring in Yellowstone National Park, USA.

Emended description of *Sphaerobacter thermophilus* Demharter *et al*. 1989

The description is as given by Demharter *et al*. (1989) with the following amendments.

Growth occurs on D-fructose and D-cellobiose but not D-xylose, D-galactose, D-mannose, D-maltose, sucrose, D-trehalose or D-raffinose. Avicel™, CMC, Phytagel™, starch and xylan act as sole carbon sources but dextrin and xanthan do not. Grows on some short alcohols including ethanol, 1-propanol, 2-propanol and mannitol but not sorbitol or methanol. Cells also grow on glycerol and sodium acetate, citrate, formate, fumarate, lactate, pyruvate and succinate. Peptone, tryptone, Casamino acids and nutrient broth act as sole carbon sources but yeast extract does not. Ammonium ion, nitrate ion or yeast extract can act as sole nitrogen sources. Growth inhibited by chloramphenicol, neomycin, kanamycin and trimethoprim, but growth is stimulated by metronidazole. Optimal growth at 55-60 °C (range: 49-67 °C) and pH 8.0-8.4 (range: 6.1-9.0). NaCl tolerance up to 1 % (w/v). The major fatty acids are 12-methyl $C_{18:0}$ and $C_{18:0}$, with minor amounts of $C_{16:0}$, 10-methyl $C_{16:0}$ and $C_{18:1}$ *n*-9. Polar lipids comprise diolPI, diolP-acylMan, diolPI-acylMan and diolPI-Man.

The type strain, *Sphaerobacter thermophilus*^{T} (=DSM 20745^T = ATCC 49802^T) was isolated from a sewage fermenter in Germany.

Emended description of *Thermomicrobium carboxidum* King and King, 2014

The description is as given by King and King (2014b) with the following amendments.

Growth inhibited by chloramphenicol, neomycin, streptomycin, and kanamycin but resistant to metronidazole and trimethoprim.

The type strain, *Thermomicrobium carboxidum*^{T} (=DSM 27067^T = ATCC BAA-2535^T) was isolated from geothermally-heated biofilm from Kilauea Iki crater (Hawai'i, USA).

Emended description of *Thermorudis peleae* King and King, 2014

The description is as given by King and King (2014b) with the following amendments.

Growth inhibited by chloramphenicol, neomycin, streptomycin, and kanamycin but resistant to metronidazole and trimethoprim. Xanthan, dextrin and CMC do not support growth.

The type strain, *Thermorudis peleae*^{T} (=DSM 27169^T = ATCC BAA-2536^T) was isolated from geothermally-heated biofilm from Kilauea Iki crater (Hawai'i, USA).

Acknowledgements

This work was supported by the Geothermal Resources of New Zealand DCF programme within GNS Science. We would like to thank the operators of Waikite Valley Thermal Pools, and Ngāti Tahu-Ngāti Whaoa Runanga Trust for their on-going support.

References

Altschul, S. F., Madden, T. L., Schäffer, A. A., Zhang, J., Zhang, Z., Miller, W. & Lipman, D. J. (1997). Gapped BLAST and PSI-BLAST: A new generation of protein database search programs. *Nucleic Acids Res*. **25**, 3389-3402.

Botero, L. M., Brown, K. B., Brumefield, S., Burr, M., Castenholz, R. W., Young, M. & McDermott, T. R. (2004). *Thermobaculum terrenum* gen. nov., sp. nov.: A non-phototrophic gram-positive thermophile representing an environmental clone group related to the *Chloroflexi* (green non-sulfur bacteria) and *Thermomicrobia*. *Arch Microbiol*. **181**, 269-277.

Carretto, L., Moore, E., Nobre, M. F., Wait, R., Riley, P. W., Sharp, R. J. & Da Costa, M. S. (1996). *Rubrobacter xylanophilus* sp. nov., a new thermophilic species isolated from a thermally polluted effluent. *Int J Syst Bacteriol*. **46**, 460-465.

Cashion, P., Holder Franklin, M. A., McCully, J. & Franklin, M. (1977). A rapid method for the base ratio determination of bacterial DNA. *Analyt Biochem*. **81**, 461-466.

Chen, M.-Y., Wu, S.-H., Lin, G.-H., Lu, C.-P., Lin, Y.-T., Chang, W.-C. & Tsay, S.-S. (2004). *Rubrobacter taiwanensis* sp. nov., a novel thermophilic, radiation-resistant species isolated from hot springs. *Int J Syst Evol Microbiol*. **54**, 1849-1855.

De la Torre, J. R., Goebel, B. M., Friedmann, E. I. & Pace, N. R. (2003). Microbial diversity of cryptoendolithic communities from the McMurdo Dry Valleys, Antarctica. *Appl Environ Microbiol* **69**, 3858-3867.

Demharter, W., Hensel, R., Smida, J. & Stackebrandt, E. (1989). *Sphaerobacter thermophilus gen. nov., sp. nov*. A deeply rooting member of the *Actinomycetes* subdivision isolated from thermophilically treated sewage sludge. *Syst Appl Microbiol*. **11**, 261-266.

Giggenbach, W., Sheppard, D., Robinson, B., Stewart, M. & Lyon, G. (1994). Geochemical structure and position of the Waiotapu geothermal field, New Zealand. *Geothermics*. **23**, 599-644.

Gladden, J. M., Allgaier, M., Miller, C. S., Hazen, T. C., VanderGheynst, J. S., Hugenholtz, P., Simmons, B. A. & Singer, S. W. (2011). Glycoside hydrolase activities of thermophilic bacterial consortia adapted to switchgrass. *Appl Environ Microbiol*. **77**, 5804-5812.

Grice, E. A., Kong, H. H., Conlan, S.& other authors (2009). Topographical and temporal diversity of the human skin microbiome. *Science*. **324**, 1190-1192.

Gupta, R., Chander, P. & George, S. (2013). Phylogenetic framework and molecular signatures for the class *Chloroflexi* and its different clades; proposal for division of the class *Chloroflexi* class. nov. into the suborder *Chloroflexineae* subord. nov., consisting of the emended family *Oscillochloridaceae* and the family *Chloroflexaceae* fam. nov., and the suborder *Roseiflexineae* subord. nov., containing the family *Roseiflexaceae* fam. nov. *Antonie van Leeuwenhoek*. **103**, 99-119.

Halebian, S., Harris, B., Finegold, S. M. & Rolfe, R. D. (1981). Rapid method that aids in distinguishing gram-positive from gram-negative anaerobic bacteria. *J Clin Microbiol*. **13**, 444-448.

Hardy, K. R. & King, G. M. (2001). Enrichment of high-affinity CO oxidizers in Maine forest soil. *Appl Environ Microbiol*. **67**, 3671-3676.

Hugenholtz, P. & Stackebrandt, E. (2004). Reclassification of *Sphaerobacter thermophilus* from the subclass *Sphaerobacteridae* in the phylum *Actinobacteria* to the class *Thermomicrobia* (emended description) in the phylum *Chloroflexi* (emended description). *Int J Syst Evol Microbiol*. **54**, 2049-2051.

Jackson, T. J., Ramaley, R. F. & Meinschein, W. G. (1973). *Thermomicrobium*, a new genus of extremely thermophilic bacteria. *Int J Syst Bacteriol*. **23**, 28-36.

Joynt, J., Bischoff, M., Turco, R., Konopka, A. & Nakatsu, C. H. (2006). Microbial community analysis of soils contaminated with lead, chromium and petroleum hydrocarbons. *Microbial Ecol*. **51**, 209-219.

Jukes, T. H. & Cantor, C. R. (1969). Evolution of protein molecules. In Mammalian protein metabolism, pp. pp. 21-132. Edited by H. N. Munro. New York: Academic Press.

Jürgens, U. J., Meißner, J., Fischer, U., König, W. A. & Weckesser, J. (1987). Ornithine as a constituent of the peptidoglycan of *Chloroflexus aurantiacus*, diaminopimelic acid in that of *Chlorobium vibrioforme f. thiosulfatophilum*. *Arch Microbiol*. **148**, 72-76.

King, C. E. & King, G. M. (2014a). Description of *Thermogemmatispora carboxidivorans* sp. nov., a carbon-monoxide-oxidizing member of the class *Ktedonobacteria* isolated from a geothermally heated biofilm, and analysis of carbon monoxide oxidation by members of the class *Ktedonobacteria*. **64**, 1244-1251.

King, C. E. & King, G. M. (2014b). Isolation and characterization of *Thermomicrobium carboxidum* KI3^T sp. nov., and *Thermorudis peleae* KI4^T gen. nov., sp. nov., novel carbon monoxide-oxidizing bacteria isolated from geothermally-heated biofilms at Kilauea Volcano, Hawaii. *Int J Syst Evol Microbiol*.

Kunisawa, T. (2011). The phylogenetic placement of the nonphototrophic, gram-positive thermophile '*Thermobaculum terrenum*' and branching orders within the phylum '*Chloroflexi*' inferred from gene order comparisons. *Int J Syst Evol Microbiol*. **61**, 1944-1953.

Lagutin, K., MacKenzie, A., Houghton, K., Stott, M. & Vyssotski, M. (2014). Novel long-chain diol phospholipids from some bacteria belonging to the class *Thermomicrobia*. *Lipids*, 1-9.

Lesaulnier, C., Papamichail, D., McCorkle, S., Ollivier, B., Skiena, S., Taghavi, S., Zak, D. & Van Der Lelie, D. (2008). Elevated atmospheric CO2 affects soil microbial diversity associated with trembling aspen. *Environ Microbiol*. **10**, 926-941.

Ludwig, W., Strunk, O., Westram, R.& other authors (2004). ARB: A software environment for sequence data. *Nucleic Acids Res*. **32**, 1363-1371.

MacKenzie, A., Vyssotski, M. & Nekrasov, E. (2009). Quantitative analysis of dairy phospholipids by ^{31}P NMR. *J Am Oil Chem Soc*. **86**, 757-763.

Meissner, J., Krauss, J. H., Jürgens, U. J. & Weckesser, J. (1988). Absence of a characteristic cell wall lipopolysaccharide in the phototrophic bacterium *Chloroflexus aurantiacus*. *J Bacteriol*. **170**, 3213-3216.

Merkel, G. J., Durham, D. R. & Perry, J. J. (1980). The atypical cell wall composition of *Thermomicrobium roseum*. *Can J Microbiol*. **26**, 556-559.

Mesbah, M., Premanchandran, U. & Whitman, W. B. (1989). Precise measurement of the G+C content of deoxyribonucleic acid by High-Performance Liquid Chromatography. *Int J Syst Bacteriol*. **39**, 159-167.

Partanen, P., Hultman, J., Paulin, L., Auvinen, P. & Romantschuk, M. (2010). Bacterial diversity at different stages of the composting process. *BMC Microbiol*. **10:94**.

Pati, A., la Butti, K., Pukall, R.& other authors (2010). Complete genome sequence of *Sphaerobacter thermophilus* type strain (S 6022^{T}) *Stand Genomic Sci*. **2**, 49-56.

Pond, J. L., Langworthy, T. A. & Holzer, G. (1986). Long-chain diols: A new class of membrane lipids from a thermophilic bacterium. *Science*. **231**, 1134-1136.

Ronquist, F., Teslenko, M., Van Der Mark, P., Ayres, D. L., Darling, A., Höhna, S., Larget, B., Liu, L., Suchard, M. A. & Huelsenbeck, J. P. (2012). MrBayes 3.2: Efficient bayesian phylogenetic inference and model choice across a large model space. *Syst Biol*. **61**, 539-542.

Schleifer, K. H. & Kandler, O. (1972). Peptidoglycan types of bacterial cell walls and their taxonomic implications. *Bacteriol Rev*. **36**, 407-477.

Schumann, P. (2011). Peptidoglycan Structure. In Methods in Microbiology, pp. 101-129. Edited by F. A. Rainey and A. Oren. Waltham, MA: Academic Press.

Sorokin, D. Y., Lucker, S., Vejmelkova, D.& other authors (2012). Nitrification expanded: discovery, physiology and genomics of a nitrite-oxidizing bacterium from the phylum Chloroflexi.

Sorokin, D. Y., Vejmelkova, D., Lücker, S., Streshinskaya, G. M., Rijpstra, W. I. C., Sinninghe Damsté, J. S., Kleerbezem, R., van Loosdrecht, M., Muyzer, G. & Daims, H. (2014). *Nitrolancea hollandica* gen. nov., sp. nov., a chemolithoautotrophic nitrite-oxidizing bacterium isolated from a bioreactor belonging to the phylum *Chloroflexi*. *Int J Syst Evol Microbiol*. **64**, 1859-1865.

Staneck, J. L. & Roberts, G. D. (1974). Simplified approach to identification of aerobic actinomycetes by thin layer chromatography. *Appl Microbiol*. **28**, 226-231.

Stott, M. B., Crowe, M. A., Mountain, B. W., Smirnova, A. V., Hou, S., Alam, M. & Dunfield, P. F. (2008). Isolation of novel bacteria, including a candidate division, from geothermal soils in New Zealand. *Environ Microbiol*. **10**, 2030-2041.

Sutcliffe, I. C. (2010). A phylum level perspective on bacterial cell envelope architecture. *Trends Microbiol*. **18**, 464-470.

Sutcliffe, I. C. (2011). Cell envelope architecture in the Chloroflexi: a shifting frontline in a phylogenetic turf war. *Environ Microbiol*. **13**, 279-282.

Suzuki, K.-i., Collins, M. D., Iijima, E. & Komagata, K. (1988). Chemotaxonomic characterization of a radiotolerant bacterium, *Arthrobacter radiotolerans*: Description of *Rubrobacter radiotolerans* gen. nov., comb. nov. *FEMS Microbiol Lett*. **52**, 33-39.

Vyssotski, M., Ryan, J., Lagutin, K., Wong, H., Morgan, X. & Stott, M. (2012). A novel fatty acid, 12,17-dimethyloctadecanoic acid, from the extremophile *Thermogemmatispora* sp. (strain T81). *Lipids*. **47**, 601-606.

Wayne, L. G., Brenner, D. J., Colwell, R. R.& other authors (1987). Report of the ad hoc committee on reconciliation of approaches to bacterial systematics. *Int J Syst Bacteriol*. **37**, 463-464.

Weisburg, W. G., Barns, S. M., Pelletier, D. A. & Lane, D. J. (1991). 16S ribosomal DNA amplification for phylogenetic study. *J Bacteriol*. **173**, 697-703.

448 **Wu, D., Raymond, J., Wu, M.& other authors (2009).** Complete genome sequence of the aerobic
449 CO-oxidizing thermophile *Thermomicrobium roseum*. *Plos One*. **4**, e4207.

450 **Yabe, S., Aiba, Y., Sakai, Y., Hazaka, M. & Yokota, A. (2011).** *Thermogemmatispora onikobensis* gen.
451 nov., sp. nov. and *Thermogemmatispora foliorum* sp. nov., isolated from fallen leaves on geothermal
452 soils, and description of *Thermogemmatisporaceae* fam. nov. and *Thermogemmatisporales* ord. nov.
453 within the class *Ktedonobacteria*. *Int J Syst Evol Microbiol*. **61**, 903-910.

454 **Ziemke, F., Höfle, M. G., Lalucat, J. & Rosselló-Mora, R. (1998).** Reclassification of *Shewanella*
455 *putrefaciens Owen's* genomic group II as *Shewanella baltica* sp. nov. *Int J Syst Bacteriol*. **48**, 179-186.

456

457

458 **FIGURE CAPTIONS**

459

460 **Figure 1.** Phylogenetic tree based on 16S rRNA gene sequences of *Thermorudis pharmacophila*
461 WKT50.2^T (highlighted) and representative isolates and environmental clones of the phylum
462 *Chloroflexi* and class *Thermomicrobia*. The tree was constructed via a Bayesian inference model
463 (MrBayes), using Markov Chain Monte Carlo (MCMC) sampling methods to calculate posterior
464 distributions of trees in the ARB software environment. Posterior probability values ≥ 90 % are
465 indicated by open circles, ≥80 % by filled circles and ≥70 % by open diamonds. The scale bar
466 represents a 0.1 change per nucleotide position.

467

468 **Figure 2**. A) Negative stain TEM image of WKT50.2^T. Scale bar = 500 nm. B) Cryo-TEM image of
469 WKT50.2^T. The insert shows an enlarged view of the cell envelope structure, CM: cytoplasmic
470 membrane; OM*: outer membrane; P*: peptidoglycan; S*: S-layer; C: Formvar-carbon support
471 mesh. Scale bar = 200 nm.*; denotes that while the Cryo-TEM shows a classical Gram-
472 negative/diderm structure, chemotaxonomic and genomic data presented in the text suggest
473 WKT50.2^T has an atypical Gram-positive monoderm-type cell envelope.

474

475

476

477

Table 1. Differential characteristics of WKT50.2^T and selected *Thermomicrobia* strains. Strains: 1, WKT50.2^T; 2, *Thermorudis peleae* KI4^T (King & King, 2014b); 3, *Thermomicrobium carboxidum* KI3^T (King & King, 2014b); 4, *Thermomicrobium roseum* DSM5159^T (Jackson *et al*, 1973; Wu *et al.*, 2009); 5, *Sphaerobacter thermophilus* DSM20745^T (Demharter *et al.*, 1989); 6, *Nitrolancea hollandicus* (Sorokin *et al.*, 2012; Sorokin *et al.*, 2014). Data generated or repeated in this study is denoted by * and # respectively.

Characteristic	1*	2	3	4	5	6
Temperature (°C)						
range	50-78	55-70	50-70	52–77*	49–67*	25-46
optimum	68-71	65	70	65–70*	55–60	40
pH						
range	6.0-8.4	5.8-8.0	6.0-9.0	6.0-9.4	6.1-9.0*	6.2–8.3
optimum	6.5-7.0	6.7-7.1	7.0	8.0-8.4*	8.0-8.4*	6.8–7.5
Pigmentation	pink	pink	off-white	pink	opaque	greenish
Gram stain	-	+#	+#	-	+	+
Catalase reaction	-	-	+	+	+	NR
Oxidase reaction	-	+	+	-	+	NR
Utilisation of:						
D-xylose	-	-	-	+*	-*	NR
D-galactose	-	-	-	+*	-*	NR
D-glucose	-	-	-	+*	-*	-
D-mannose	-	-	-	+*	-*	NR
D-fructose	-	-	-	+*	+*	-
sucrose	+	-	-	+	-*	NR
glycerol	+	-	-	+	+*	NR
Avicel™	+	+	+	-*	+*	NR
CMC	+	-*	NR	-*	+*	NR
dextrin	-	-*	NR	+*	-*	NR
xanthan	-	-*	NR	+*	-*	NR

yeast extract	+	-	-	+	-*	-
CO	-	-	+	+	+*	-
Antibiotic resistance	las†, met†, tri†	met*, tri*	met*, tri*	chl, met†*, str, tri†*	met†*	NR
Primary fatty acids	12-methyl $C_{18:0}$, $C_{18:0}$	12-methyl $C_{18:0}$	12-methyl $C_{18:0}$	12-methyl $C_{18:0}$, $C_{18:0}$	12-methyl $C_{18:0}$, $C_{18:0}$*	12-methyl $C_{18:0}$
Primary quinones	MK-8, MK-9	NR	NR	MK-8, MK-8 2,3-epoxide*	MK-8	MK-8
G+C content (mol%)	58.4	60.7	66.0	64.3	66.0	62.6

+, positive; -, negative; NR, not reported.

† stimulates growth; chl, chloramphenicol; las, lasalocid A; met, metronidazole; str, streptomycin; tri, trimethoprim

Figure 1

Click here to download Figure: Figure_1_phylogenetic tree.jpg

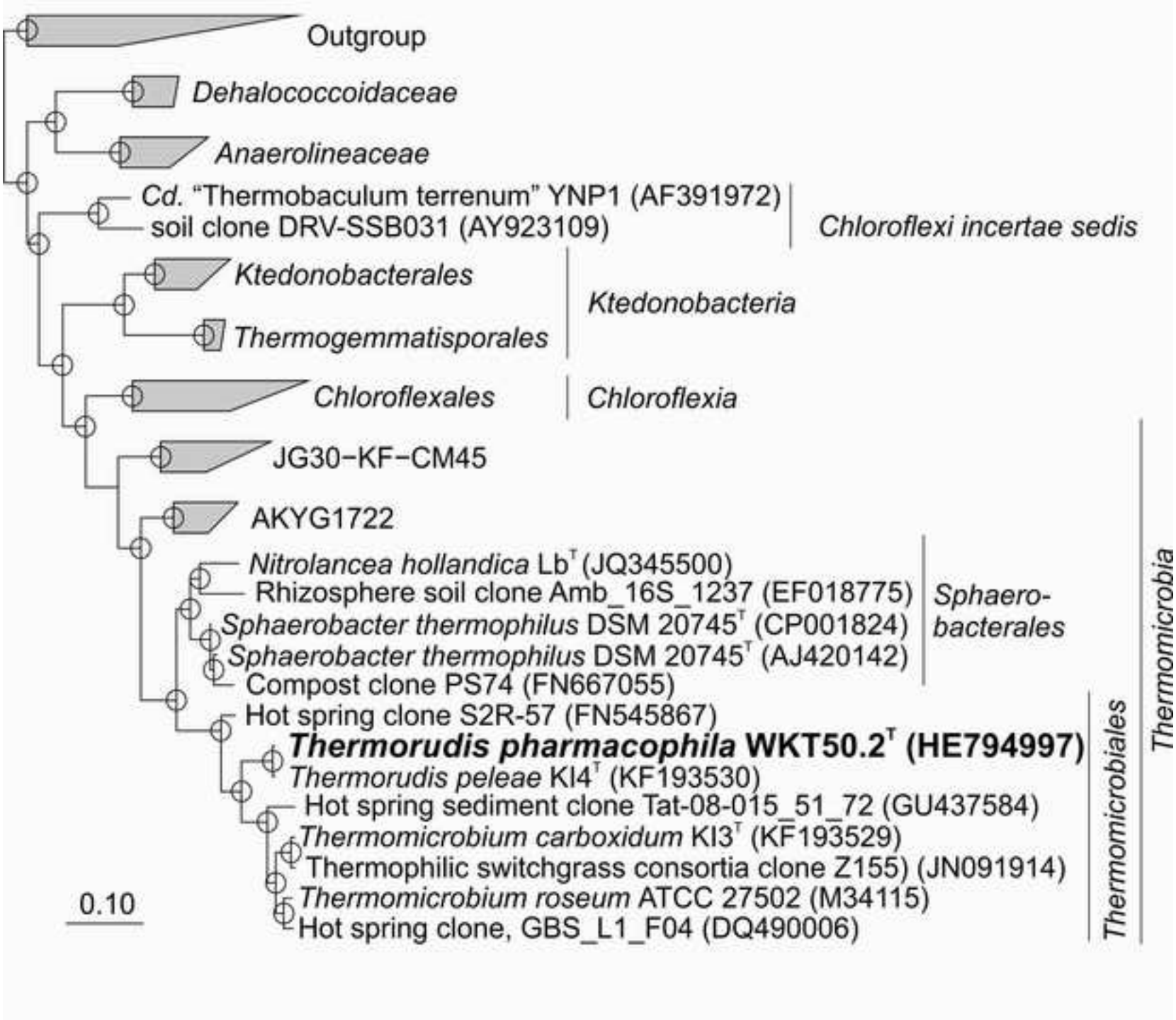

Figure 2
Click here to download Figure: Figure 2_TEM.jpg

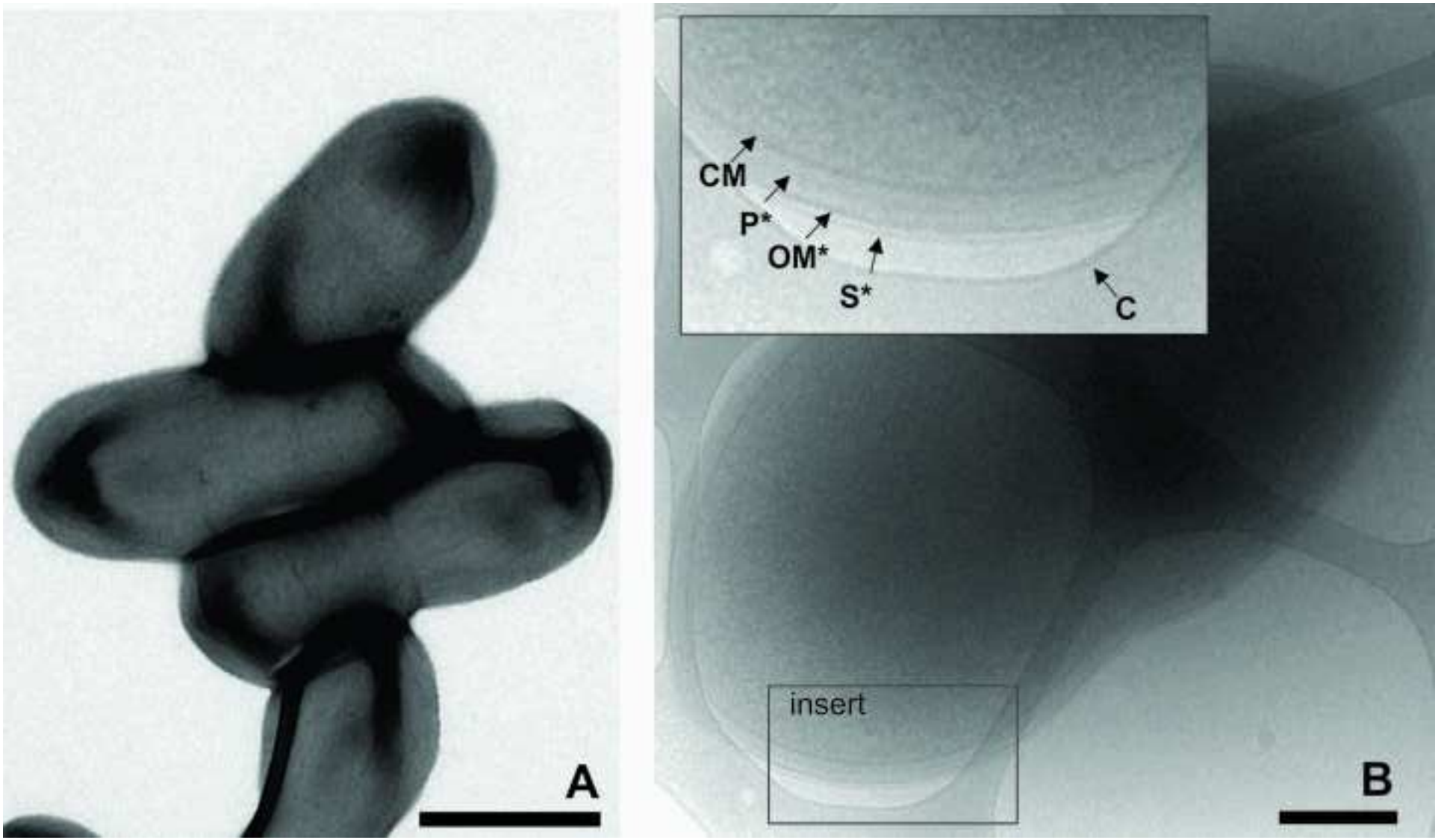

International Journal of Systematic and Applied Microbiology

SUPPLEMENTARY INFORMATION

Manuscript Title:

***Thermorudis pharmacophila* WKT50.2^T sp. nov., a novel isolate of class *Thermomicrobia* isolated from geothermal soil, and emended descriptions of *Thermomicrobium roseum*, *Thermomicrobium carboxidum*, *Thermorudis peleae* and *Sphaerobacter thermophilus*.**

Karen M. Houghton[1,2], Xochitl C. Morgan[3], Kirill Lagutin[4], Andrew D. MacKenzie[4], Mikhail Vyssotskii[4], Kevin Mitchell[4], Ian R. McDonald[2], Hugh W. Morgan[2], Jean F. Power[1], John W. Moreau[5], Eric Hanssen[5] and Matthew B. Stott[1]

[1]GNS Science, Extremophiles Research Group, Private Bag 2000, Taupō, 3352, New Zealand
[2]School of Science, University of Waikato, Private Bag 3105, Hamilton 3240, New Zealand
[3]Department of Biostatistics, Harvard T. H. Chan School of Public Health, 655 Huntington Ave., Boston MA 02115, USA
[4]Callaghan Innovation, PO Box 31310, Lower Hutt 5040, New Zealand
[5]University of Melbourne, 30 Flemington Road, Victoria 3010, Australia

Corresponding author: m.stott@gns.cri.nz

MATERIALS AND METHODS

General

Unless otherwise stated, the following methodology was used for all media. The pH of all media was adjusted prior to sterilisation with either 1 M NaOH or 1 M H_2SO4. Medium pH was measured at room temperature using a PHM250 Ion Analyser pH probe (Radiometer Analytical SAS, Lyon, France). Crimp-top serum bottles or Schott™ bottles were filled such that the medium to headspace ratio was approximately 1:1. The headspace was always aerobic unless otherwise stated, and the bottles were sealed with butyl rubber septa prior to sterilisation. All media were autoclaved at 121 °C and 15 lb/in^2 for 20 min using a P52014 Pressure Vessel (Mercer Stainless Limited, Henderson, New Zealand) and were stored at 4 °C. Solid media were aseptically transferred immediately after sterilisation at about 80 °C into sterile petri dishes and allowed to solidify. Growth was determined via optical density at 600 nm (OD_{600}) using 1 ml polystyrene cuvettes with a pathlength of 1 cm

(Thermo Fisher Scientific Inc., Waltham, USA) or a 17 mm test tube holder (Perkin Elmer) on a HALO VIS-10 Spectrometer (Dynamica, Australia).

Phenotypic testing

General. All substrate utilisation tests were performed using minimal medium (Castenholz salts solution (Ramaley *et al.*, 1970): detailed below) without any energy source. All other metabolic testing was conducted using Castenholz salts solution with the addition of 0.5 g l^{-1} peptone and 0.25 g l^{-1} sucrose (CPS), or 5 g l^{-1} peptone and 2.5 g l^{-1} sucrose (10x CPS). Inoculum for phenotypic determination was generated by growing cells in 10x CPS for 2-3 days. Cells were cultured in triplicate in 125 ml serum bottles sealed with rubber butyl septa, and containing an aerobic headspace to medium ratio of 1:1. Cells were incubated in an orbital incubator at 68 °C (WKT50.2^{T} and *T. roseum)* or 55 °C (*S. thermophilus)* and 130 r.p.m., and growth was determined based on the fastest growth rate and highest OD_{600} obtained. For all tests, a negative control with no carbon/energy source and a positive control using the standard growth medium were applied in parallel.

Castenholz salts solution (Ramaley *et al.*, 1970)

Nitrilotriacetic acid	0.1 g l^{-1}
$MgSO_4.7H_2O$	0.1 g l^{-1}
$CaCl_2.2H_2O$	0.06 g l^{-1}
NaCl	0.008 g l^{-1}
$NaNO_3$	0.689 g l^{-1}
KNO_3	0.103 g l^{-1}
$Na_2HPO_4.12H_2O$	0.111 g l^{-1}
$FeCl_2$ solution	1 ml l^{-1}
Nitsch element solution	1 ml l^{-1}

$FeCl_2$ Solution

$FeCl_2.4H_2O$	0.44 g l^{-1}

Nitsch Element Solution

Concentrated H_2SO_4	0.5 ml l^{-1}
$MnCl_2.4H_2O$	2.8 g l^{-1}
$ZnSO_4.7H_2O$	0.5 g l^{-1}
H_3BO_3	0.5 g l^{-1}
$CuSO_4.5H_2O$	0.16 g l^{-1}
$Na_2MoO_4.2H_2O$	0.03 g l^{-1}
$CoCl_2.6H_2O$	0.046 g l^{-1}

TEM analysis. Transmission Electron Microscopy (TEM) was performed at the Bio21 Institute Advanced Microscopy Facility, University of Melbourne, Australia. Two different methods were applied to visualise cells in exponential growth phase:

i) For negative staining, cells were absorbed on a glow-discharged formvar carbon-coated 400-mesh copper grid, and stained with 2 % (w/v) uranyl acetate. The resulting grids were observed on a FEI Tecnai F20 operating at 200 kV and digital micrographs were recorded with a Gatan Ultrascan 1000.

ii) For cryoTEM, cells were absorbed on glow discharge holey carbon grids and plunge frozen in liquid ethane. The resulting grids were observed on a FEI Tecnai F30 operating at 300 kV under low dose. Each micrograph was recorded on a Gatan Ultrascan 1000 with a total dose of ~2,000 $e^- nm^{-2}$.

Fatty acids analysis. Cells were prepared for fatty acid analysis by combining cell biomass from 2 l of 10x CPS enrichment grown aerobically at 68 °C (WKT50.2^T and *T. roseum*) or 55 °C (*S. thermophilus*) at 130 r.p.m. Lipids were extracted from wet biomass (Bligh and Dyer, 1959) and methylated (Carreau *et al.*, 1978). GC analysis of fatty acid methyl esters was performed on a TraceGC Ultra instrument (ThermoFinnigan, USA), equipped with a FID and TG WaxMS (30 m × 0.25 mm i.d., 0.25 µm) capillary column (ThermoFinnigan, USA). Helium was used as the carrier gas; the split ratio was 1:100. The oven temperature was 190 °C. The injector and detector temperatures were 280 °C. Samples were reanalysed on a GCMS-QP2010Ultra (Shimadzu) equipped MS detector and TG WaxMS (30 m × 0.25 mm i.d., 0.25 µm) capillary column (ThermoFinnigan, USA) to confirm fatty acid structural assignments. Helium was used as the carrier gas; the split ratio was 1:30. Separation temperature was 200 °C. Injector temperature was 280 °C. Fatty acids were identified by equivalent chain length (ECL) values (Stránský *et al.*, 1992), mass spectra, and comparison with fatty acid mixtures of known composition derived from other bacteria.

Polar lipid analysis. Total cellular lipids were extracted from the biomass using as previously described (Bligh *et al.*, 1959). Polar lipids were separated by two-dimensional thin layer chromatography (silica gel, Macherey-Nagel Art. No. 818 033, cut to 10 x 10 cm). The first direction was developed in chloroform: methanol: water (65:25:4, v/v/v), and the second in chloroform: methanol: acetic acid: water (80:12:15:4, v/v/v/v) (Figure S1) (Tindall *et al.*, 2007). Primary amines were detected with 0.2 % (w/v) ninhydrin in absolute ethanol. Phospholipids were detected with the molybdite spray reagent (Vaskovsky *et al.*, 1975). Glycolipids were detected with 0.5 % (w/v) anthrone in toluene. Another duplicate plate was charred by spraying with 10 % (v/v) sulfuric acid in methanol and incubating at 120 °C for 30 min, in order to show total lipids. Phospholipid classes in the extract were observed using ^{31}P NMR (MacKenzie *et al.*, 2009).

Anaerobic growth. Cells were grown in a modified Castenholz salts solution with nitrate replaced by 0.58 g l^{-1} NH_4Cl, and $MgSO_4.7H_2O$ replaced with 0.08 g l^{-1} $MgCl_2.6H_2O$. Sucrose (2.5 g l^{-1}) was used as a carbon source for WKT50.2^T and *T. roseum*, and fructose (2.5 g l^{-1}) for *S. thermophilus*. Anaerobic growth was tested using either elemental S^0 (6.5 g l^{-1}), Na_2SO_4 (0.5 g l^{-1}) or $NaNO_3$ (0.5 g l^{-1}). Resazurin (1 mg l^{-1}) and $Na_2S.9H_2O$ (1 mM) were added to the medium, as an anaerobic indicator and reducing agent respectively, prior to sterilisation. The headspace comprised (v/v): 85 % N_2, 10 % H_2 and 5 % CO_2. Vials were incubated at 65 °C for WKT50.2^T and *T. roseum*, 55 °C for *S. thermophilus*.

Temperature range and optimum determination. Cells were grown in 10 ml medium in 27 ml anaerobic tubes sealed with butyl rubber stoppers. Headspaces were aerobic. The tubes were incubated in duplicate in a temperature gradient incubator (Terratec Corporation, Hobart, Australia) set from 49 °C to 84 °C and agitated at 30 oscillations per min. There were 24 tubes over the temperature range with an average of 1.5 °C between each subsequent tube.

pH range and optimum determination. The pH growth range was determined by growing cells in buffered 10x CPS liquid medium between pH 4.5 and 9.2. The buffers used were acetate (buffer range pH 4.5-6.5) or Tris (buffer range pH 6.9-9.2). pH was measured after sterilisation and inoculation.

Salt tolerance. Cells were grown in 10x CPS, with the addition of either 0.5, 1, 2, 3, 4 or 5 % (w/v) NaCl. Growth was determined by the visible formation of biomass and measurement of OD_{600} nm.

Preferred N-source. The preferred nitrogen source was determined using a modified version of Castenholz salts solution without $NaNO_3$ or KNO_3, and sucrose or fructose (0.5 g l^{-1}) as carbon source. Initially, dinitrogen gas as an N-source was tested by incubating strains in Castenholz salts medium minus KNO_3. As no N_2-fixation was observed, no manipulation of the headspace was required to test alternate N-sources. Nitrogen sources tested were either KNO_3 (0.689 g l^{-1}), $(NH_4)_2SO_4$ (1.48 g l^{-1}), KNO_2 (1.7g l^{-1}), urea (0.23 g l^{-1}), alanine (0.70 g l^{-1}), serine (0.80 g l^{-1}), trimethoprim (30 µg ml^{-1}), or metronidazole (30 µg ml^{-1}). All nitrogen sources were added after sterilisation by aseptically passaging them into the medium via a 0.22 µm syringe filter.

Carbon monoxide utilisation. The induced oxidation of carbon monoxide was determined using a method previously described (Hardy *et al.*, 2001). WKT50.2^T cells were grown in Castenholz salts solution with 0.05 % (w/v) yeast extract. The headspace contained 100 ppm of CO in air. For testing constitutive oxidation, cells were grown in 10x CPS media initially with an aerobic headspace, then 100 ppm of CO was added once cells had grown to form visible biomass. For CO analysis, gas samples were removed from vials and analysed immediately using a Peak Performer 1 Gas Analyser (Peak Laboratories, Mountain View, C.A., USA) equipped with Unibeads 1S and Molecular Sieve 13X columns, and a Reducing Compound Photometer. The temperature was set at 105 °C, and compressed air was used as a carrier. Detection limits were about 2 ppm. The instrument was standardized using a certified CO standard (1044 ppm, Airgas Gulf States, Theodore, USA), and laboratory dilutions of this standard.

PCR was performed using primers specific to the large subunit of carbon monoxide dehydrogenase genes (King, 2003) to amplify putative *coxL* fragments. Further primer pairs (Table S5) were designed on the basis of conserved motifs, including the active site, using the genomes of *T. roseum* (http://www.ncbi.nlm.nih.gov/nuccore/NC_011959.1) and *S. thermophilus* (http://www.ncbi.nlm.nih.gov/nuccore/NC_013524.1), using Geneious version 6.0.5 (Biomatters, http://www.geneious.com/). PCR was carried out in 50 µl reaction volumes in 200 µl tubes containing 100 µM dNTPs, 0.5 µM primers and 1U Intron i-Taq™. The final concentration of $MgCl_2$ was 1.5 mM. DNA extracts from cultures were used at final concentrations of 10-50 ng. The PCR conditions were as follows: 94 °C for 3 min; 10 cycles consisting of 94 °C for 45 sec, 62 °C for 60 sec, with a 1 °C decrease every 2 cycles, and 72 °C for 90 sec; 30 cycles consisting of 94 °C for 45 sec, 58 °C for 60 sec and 72 °C for 90 sec; and a final elongation step at 72 °C for 20 min. PCR amplifications were performed using a CGI-96 thermal cycler (Corbett Research, Sydney, Australia) with PalmCycler™ software, v2.1.10.

Extraction of respiratory quinones. Respiratory quinones were extracted using a modified version of the method described by Nishijima and colleagues (Nishijima *et al*., 1997). Briefly, approximately 5-30 mg of freeze dried cell material was ground to a fine powder using a mortar and pestle and extracted by addition of 2:1 chloroform/methanol. The resultant solution was ultrasonicated at room temperature for 15 min then filtered through a 0.2 µm nylon syringe filter. The filtered solution was dried under a stream of nitrogen and dissolved in in acetone prior to analysis by LCMS.

Analysis of respiratory quinones. Analysis of extracts were carried out using a modified version of the method described by Nishijima and colleagues (Nishijima *et al*., 1997). Extracts dissolved in acetone were analysed by LCMS on a system comprising of a Shimadzu 8040_LCMS system equipped with photodiode array detector and triple quadrapole low resolution MS utilising an APCI source for ionisation. High resolution MS by direct infusion was carried out on a Waters Premier QTof instrument. LCMS chromatography was carried out on a Waters Acquity BEH C18 1.7 µm, 2x150 mm column at 30 °C. A linear gradient elution profile was employed. The initial elution condition was 100 % methanol, which was held for 1 min. At 4 min, 2-propanol was injected to 5 % (v/v), then the concentration increased at a linear rate to 100 % 2-propanol at 22 min, and held at this concentration for 1 min before being reduced to initial conditions over 1 min. The column was equilibrated for 7 min prior to a subsequent injection being made. A flow rate of 0.2 ml min^{-1} was employed. The class of respiratory quinones assigned to observed peaks in the UV-Vis and MS TIC chromatograms were determined from a combination of their characteristic UV-Vis online absorption spectra and their characteristic MS/MS fragmentation patterns. The number of isoprene units for each quinone observed was determined from their retention times, with reference to quinone peaks

observed in chromatograms of microbial extracts of known composition, and their low resolution *m/z* values indicating chain length.

The unique respiratory quinone peak observed in *T. roseum* extracts was tentatively identified as MK-8 2,3-epoxide via a range of methodologies and observations: LCMS analyses of the *T. roseum* extract (Fig. S4) showed the compound's peak eluted earlier than that of MK-8 (recorded at 270 nm). The peak had a low resolution mass of 733 *m/z* [M+H]+ which suggested that the compound was 16 mass units greater than MK-8. High resolution MS analysis of a quinone-rich extract of *T. roseum* by direct infusion MS indicated a molecular formula of $C_{44}H_{77}O_8$ [M+H]+, consistent with presence of an additional oxygen. The observation that the UV absorption spectrum of the unknown compound (absorption maxima observed at 227, 265 sh, 303 nm - Fig. S5), was distinct from that of MK-8 (absorption maxima observed at 249, 263 sh, 270 nm - Fig. S6), suggested that the additional oxygen substitution was to the main quinone ring rather than to the isoprene tail. An extract of *S. thermophilus*, which almost exclusively produces MK-8, underwent epoxidation following the method reported for epoxidation of MK-4 to MK-4 2,3-epoxide (Suhara, 2010). The resultant reaction solution gave a single quinone peak on LCMS that had a low resolution mass of 733 *m/z* [M+H]+, and a similar on-line UV absorption spectrum to that of the unknown peak. When the *T. roseum* extract was mixed with the epoxidation reaction mixture and injected onto the LCMS it was found that both peaks co-eluted as a single peak. These results support the hypothesis that the structure of the unknown quinone is MK-8 2,3-epoxide.

As an analytical standard of MK-8 2,3-epoxide was not available for comparison, the relative levels of quinones in *T. roseum* were determined by comparison of peak areas in the UV chromatograms recorded on the LCMS. For relative levels of MK-8 and the putative MK-8 2,3 epoxide, peak areas at 248 nm (KM-8) and 266 nm (MK-8 2,3 epoxide) were compared with reference to the molar extinction coefficients published for MK-4 and MK-4 2,3 epoxide at these wavelengths (Sherman 1981). For relative levels of MK-8 and MK-9, it was assumed that the molar extinction coefficients for both compounds at 270 nm were the same (Nishijima *et al.*, 1997).

Genome screening for enzymes involved in cell envelope synthesis and function. The draft WKT50.2^T genome was screened for genes encoding proteins involved in plasma membrane translocation, and for genes involved in secretory systems and biosynthesis of the outer membrane. The gene presence / absence analysis was undertaken via word search in the RAST server (Aziz *et al.*, 2008). Key protein family domains genes were referenced as per Sutcliffe (2011 – see below).

213 Representative Pfam domains for proteins associated with plasma membrane translocation pathways,
214 and secretions systems and outer membranes. Adapted from Sutcliffe (2011). Presence of gene
215 indicated by 'Y', absence 'N'.

System	**Cellular location**	**Pfam domain**	**WKT50.2^T**
Tat translocon	Plasma membrane	Pf00902	Y
Lipoprotein biogenesis	Plasma membrane	Pf01790	Y
	Plasma membrane	Pf01252	Y
Sec tranlocon	Plasma membrane	Pf00344	Y
Outer membrane assembly	Outer membrane Periplasm	Pf07244 & Pf01103 Pf00847	N
Secretion systems *			
T1SS	Outer membrane & Periplasm	Pf02321	N
T2SS, T3SS	Outer membrane	Pf00263	N
	Outer membrane	Pf03958	N
	Outer membrane	Pf07660	
T4SS	Outer membrane	Pf03524	N
	Periplasm/plasma membrane	Pf04335	N
	Periplasm/plasma membrane	Pf03743	N
T5aSS	Outer membrane	Pf03797	N
T5bSS	Outer membrane	Pf03865	N
T5cSS	Outer membrane	Pf03895	N
T6SS	Tubule	Pf05638	N
T7SS	Outer membrane	Pf00577	N
T8SS	Outer membrane	Pf10614	N

216 * Secretion systems nomenclature as per Desvaux *et al*., 2009.
217

SUPPLEMENTARY TABLES

Table S1. Fatty acid composition of WKT50.2^T and *S. thermophilus* in weight % of total fatty acids. Only components > 0.5 % are presented.

Saturated fatty acids	WKT50.2^T	*S. thermophilus*
$C_{14:0}$	1.2	1.5
$C_{16:0}$	5.4	9.5
$C_{18:0}$	30.6	17.1
$C_{20:0}$	7.3	-
Unsaturated fatty acid		
$C_{18:1}$ *n*-9*	-	2.3
Methyl-branched fatty acids		
10-methyl $C_{16:0}$*	1.5	5.5
12-methyl $C_{17:0}$*	-	0.9
12-methyl $C_{18:0}$*	54.0	63.2

* - *positions of unsaturation and branching were identified by GCMS.*

Table S2. Polar lipids of WKT50.2^T and *S. thermophilus*

	WKT50.2^T	*S. thermophilus*
Phospholipids	mol%	
diolP-acylMan	17.9	17.0
diolPI-Man	6.7	33.3
diolPI-acylMan	11.5	8.4
diolPI	64.0	41.3
1,2-diols	% 1,2-diols	
11-methyl $C_{17:0}$	-	0.8
13-methyl $C_{18:0}$	-	4.4
n19:0	15.2	20.2
13-methyl $C_{19:0}$	26.0	66.2
$C_{21:0}$*br*	-	3.3
n20:0	1.2	0.2
13-methyl $C_{20:0}$	0.3	0.7
n21:0	50.6	-
15-methyl $C_{21:0}$	1.4	-

227 **Table S3.** Substrate utilisation of WKT50.2^T, *S. thermophilus* and *T. roseum*. Substrates at 0.2 %
228 unless otherwise stated.
229

Group	Substrate	WKT50.2^T	*S. thermophilus*	*T. roseum*
Monosaccharides	DL-arabinose	-	ND	ND
	D-fructose	-	+	+
	L-fucose	-	ND	ND
	D-galactose	-	-	+
	D-glucose	-	-	+
	D-mannose	-	-	+
	rhamnose	-	ND	ND
	D-ribose	-	ND	ND
	D-xylose	-	-	+
Disaccharides	D-cellobiose	-	+	+
	lactose	-	ND	ND
	D-maltose	-	-	+
	sucrose	+	-	+
	D-trehalose	+	-	+
Trisaccharide	D-raffinose	+	-	+
Sugar derivatives	D-galacturonic acid	-	ND	ND
	D-glucuronic acid	-	ND	ND
	D-N-acetylglucosamine	-	ND	ND
Glucose-based polymers	Avicel™	+	+	-
	CMC	+	+	-
	dextrin	-	-	+
	starch	+	+	+
	Whatman™ filter paper	±	ND	ND
Algal and plant-derived polymers	agarose	-	ND	ND
	sodium alginate	+	ND	ND
	galactomannan	-	ND	ND
	glucomannan	-	ND	ND
	lignin	-	ND	ND
	pectin	-	ND	ND
	xylan	+	ND	ND
Bacterial exopolysaccharides	Phytagel™	-	+	+
	xanthan	-	-	+
Animal-derived polymers	chitin	-	ND	ND
Organic salts	sodium acetate	+	+	+
	trisodium citrate	-	+	+
	sodium formate	+	+	+
	sodium fumarate	+	+	+
	sodium lactate	+	+	+
	sodium pyruvate	+	+	+
	sodium succinate	+	+	+

++ very good growth; + growth; ± weak growth; - no growth; ND, not determined

Group	Substrate	WKT50.2^T	*S. thermophilus*	*T. roseum*
Alcohols (0.05 %)	methanol	+	-	+
	ethanol	+	+	+
	1-propanol	-	+	+
	2-propanol	-	+	+
Sugar alcohols	sorbitol	+	-	-
	mannitol	-	+	+
Protein derivatives / amino acids	yeast extract	+	-	+
	peptone	++	+	+
	tryptone	+	+	+
	Casamino acids	+	+	+
	alanine	-	ND	ND
	cysteine	-	ND	ND
	glutamic acid	-	ND	-
	glycine	-	ND	ND
	leucine	-	ND	ND
	lysine	-	ND	ND
	methionine	-	ND	ND
	serine	-	ND	ND
	tryptophan	-	ND	ND
	valine	-	ND	ND
Others	B-vitamins (Stott *et al.*, 2008)	-	ND	ND
	sodium benzoate	-	ND	ND
	ascorbic acid	-	ND	ND
	glycerol	++	+	+
	methylamine (0.05 %)	-	ND	ND
	trimethylamine (0.05 %)	-	ND	ND
	trimethoprim (30 µg ml^{-1})	-	ND	ND
	metronidazole (30 µg ml^{-1})	-	ND	ND
	Nutrient broth	+	+	ND
	R2A	+	ND	+

++ very good growth; + growth; ± weak growth; - no growth; ND, not determined;

Table S4. Primer sequences for coxL amplification

Name	Sequence 5' – 3'
OMPf *	GGC GGC TTY GGS AAS AAG GT
BMSf *	GGC GGC TTY GGS TCS AAG AT
O/Br*	YTC GAY GAT CAT CGG RTT GA
cox F1	TAC GTC GAC GAC GTC AAA CT
cox F2	GTC GAG TAC GAG CCG CTG
cox R1	CAR GGG CAG GGA CAC GAG AC
cox R2	TTY GCS GCC TAC ACG AAT TTC CCG C
Thermo cox F	TGC CGG TCT ACC CCG GCT AC
Thermo cox R	CTG TCG TAC TCC CAG CCG GT

*previously published (King, 2003).

Table S5 – Growth response to metronidazole and trimethoprim of WKT50.2^T, *S. thermophilus* and *T. roseum*

Antibiotic	% growth compared to positive control*		
	WKT50.2^T	*S. thermophilus*	*T. roseum*
metronidazole (3 μg ml^{-1})	113	39	196
metronidazole (30 μg ml^{-1})	343	105	202
trimethoprim (3 μg ml^{-1})	119	13	121
trimethoprim (30 μg ml^{-1})	135	2	134

*The mean OD_{600} of three test cultures was compared to the mean of three controls, and the result is expressed as a percentage of growth compared to the control.

Table S6. api®ZYM strips (bioMérieux) - selected enzyme activity for WKT50.2^T

Positive activity	**Weak or no activity**
esterase (C4)	alkaline phosphatase
esterase lipase (C8)	cysteine arylamidase
lipase (C14)	α-chymotrypsin
leucine arylamidase	acid phosphatase
valine arylamidase	naphthol-AS-BI-phosphohydrolase
trypsin	α-galactosidase
	β-galactosidase
	β-glucuronidase
	α-glucosidase
	β-glucosidase
	N-acetyl-β glucosaminidase
	α-mannosidase
	α-fucosidase

SUPPLEMENTARY FIGURES

Figure S1.

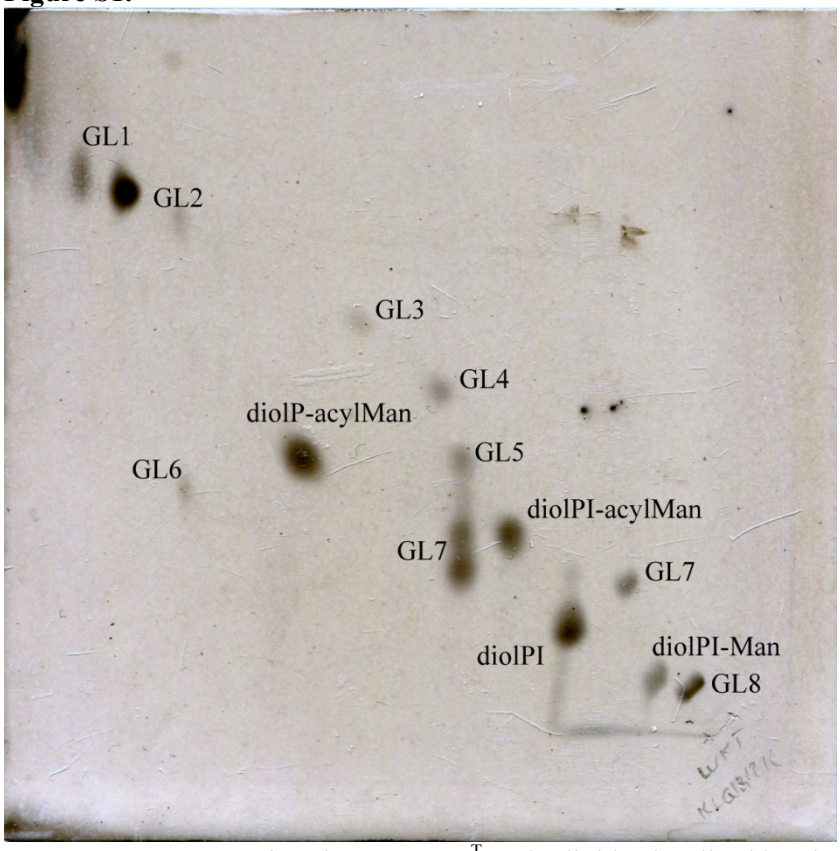

Figure S1. 2D-TLC of strain WKT50.2^{T}, polar lipids visualised by charring after spraying with 10 % v/v sulphuric acid in methanol. The first development is the vertical axis (bottom to top) and the second development is the horizontal axis (right to left). GL – a glycolipid.

Figure S2.

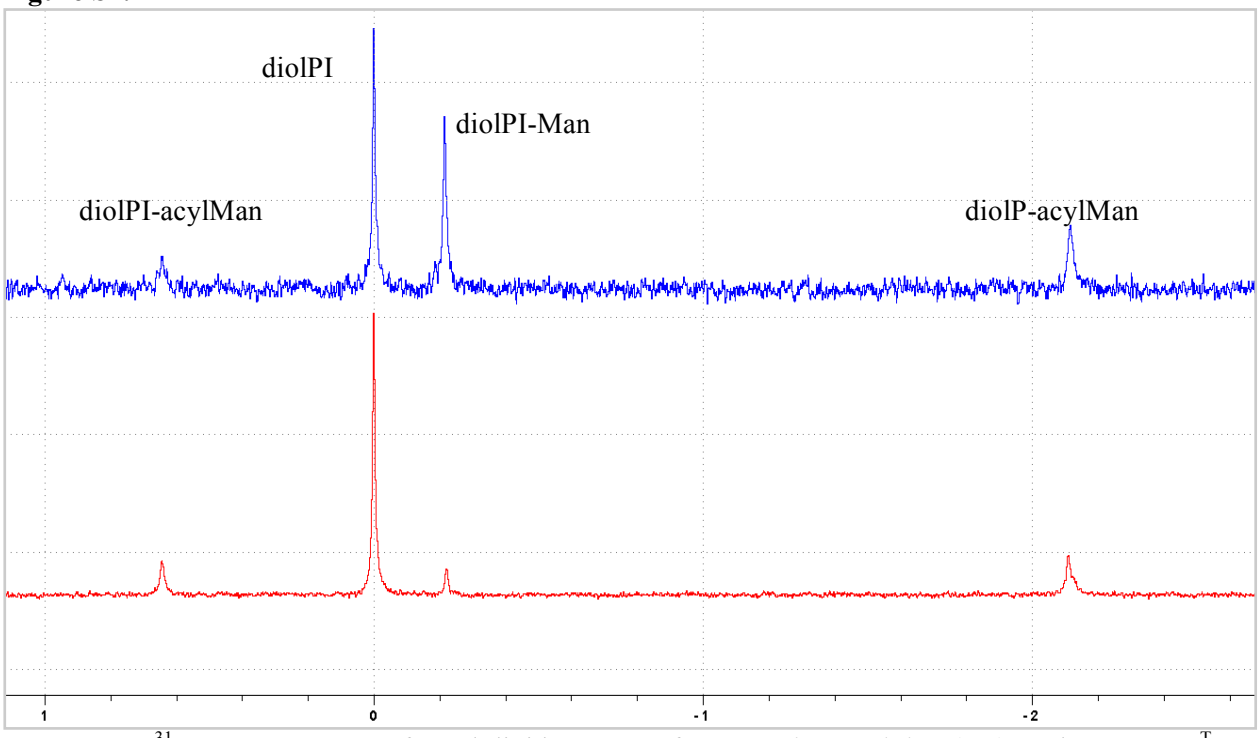

Figure S2. ^{31}P NMR spectra of total lipid extracts from *S. thermophilus* (top) and WKT50.2^{T} (bottom). The lipid extracts were dissolved in 10 % (w/w) sodium cholate, 1 % EDTA (w/w), aqueous NMR detergent (80:20 v/v H_2O:D_2O, pH 7.2). Chemical shifts are relative to a 0.4 % (v/v) phosphoric acid solution in a capillary insert.

Figure S3.

A

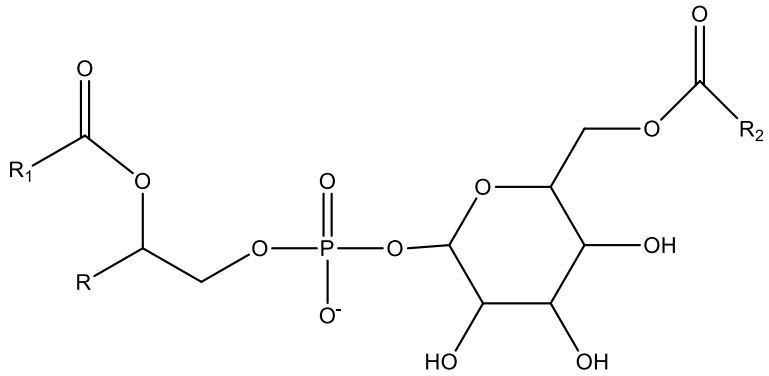

B

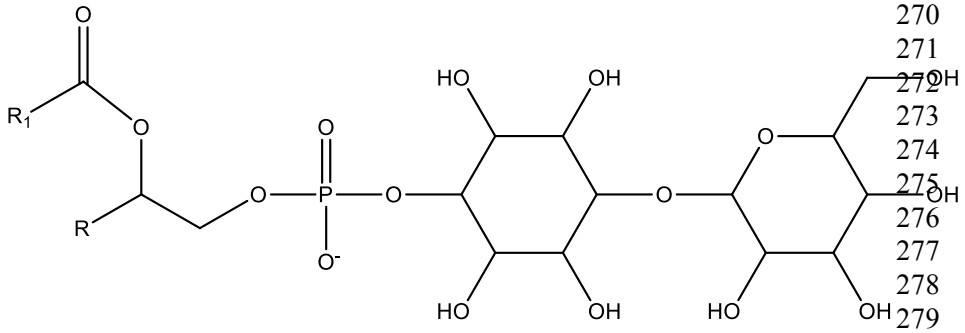

C

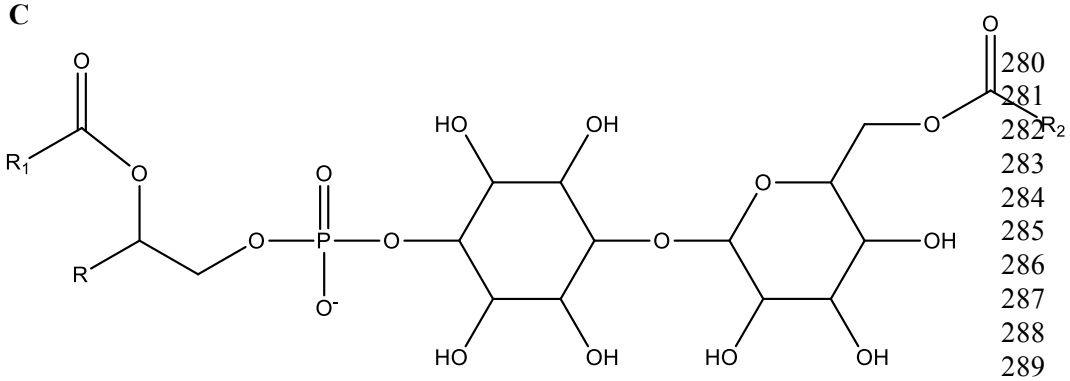

D

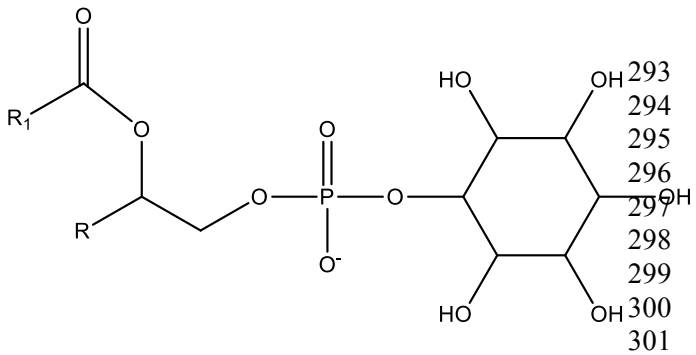

Figure S3 A-D. Structures of the novel 1,2-diol based phospholipids found in WKT50.2^{T} and *S. thermophilus*. A) diol-phosphatidyl acylmannoside (diolP-acylMan), B) diol-phosphatidylinositol mannoside (diolPI-Man)*, C) diol-phosphatidylinositol acylmannoside (diolPI-acylMan)*, D) diol-phosphatidylinositol (diolPI). *The attachment position of the sugar to the inositol was not studied.

306

307 **Figure S4**

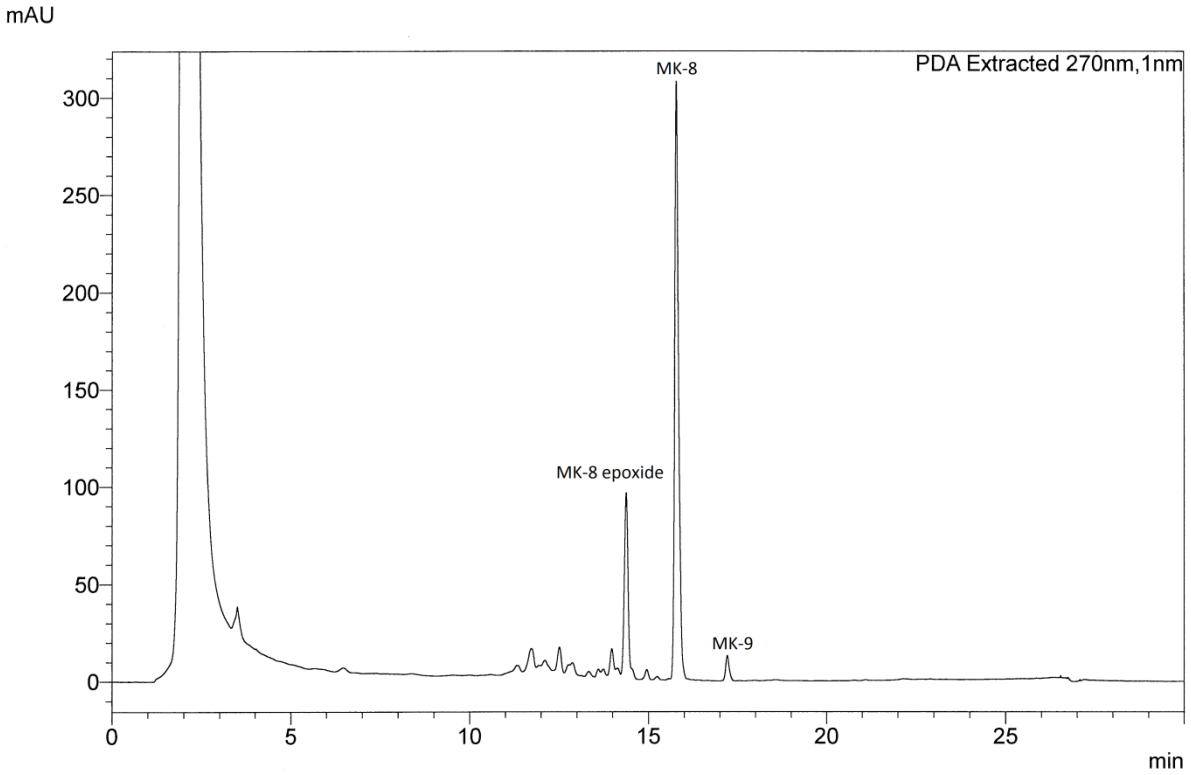

308

309 **Figure S4.** LCMS chromatogram of *T. roseum* extract recorded at 270 nm showing the three assigned
310 quinone peaks, MK-8 2,3-epoxide, MK-8, and MK-9.

311

Figure S5

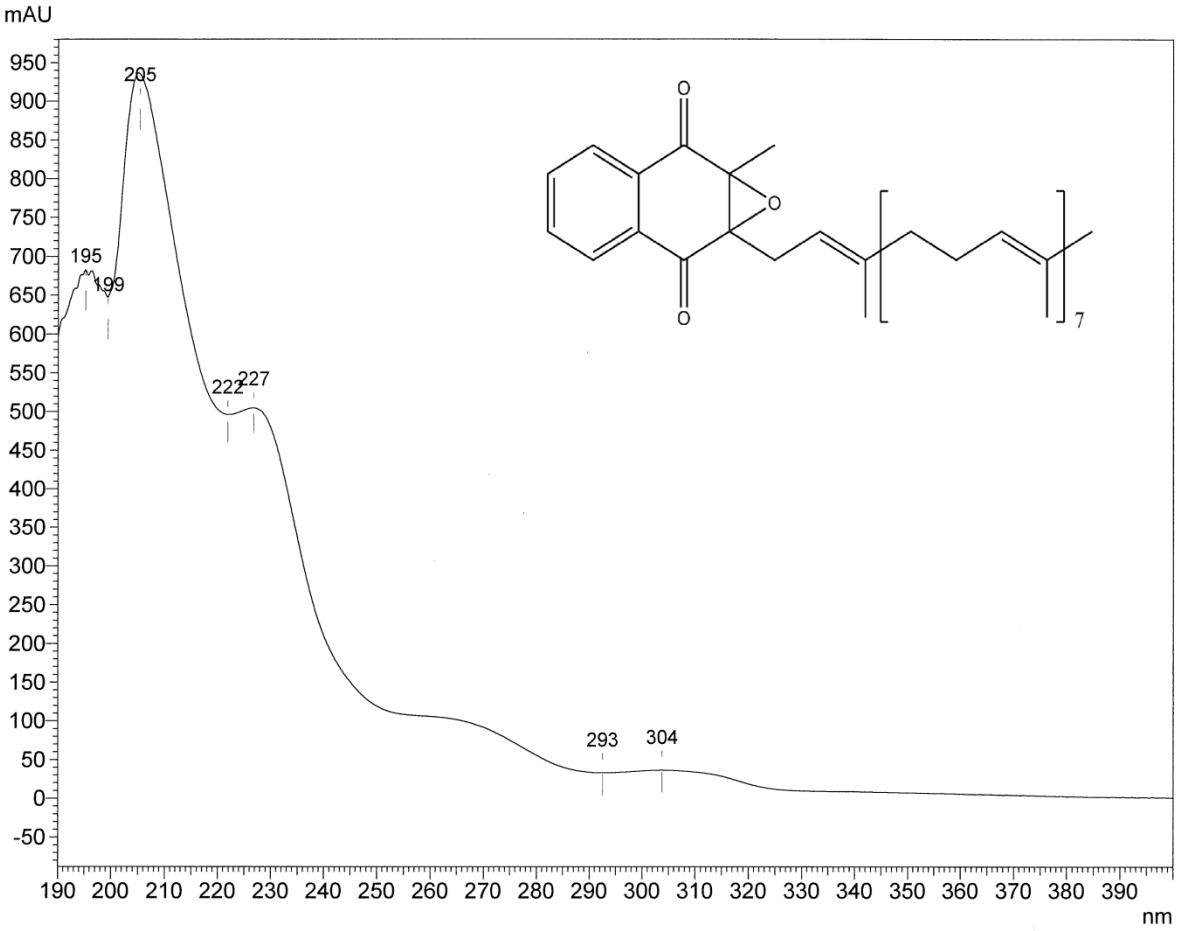

Figure S5. LCMS On-line UV-visible absorption spectrum of the peak proposed to be MK-8 epoxide and the suggested structure of MK-8 2,3-epoxide.

Figure S6

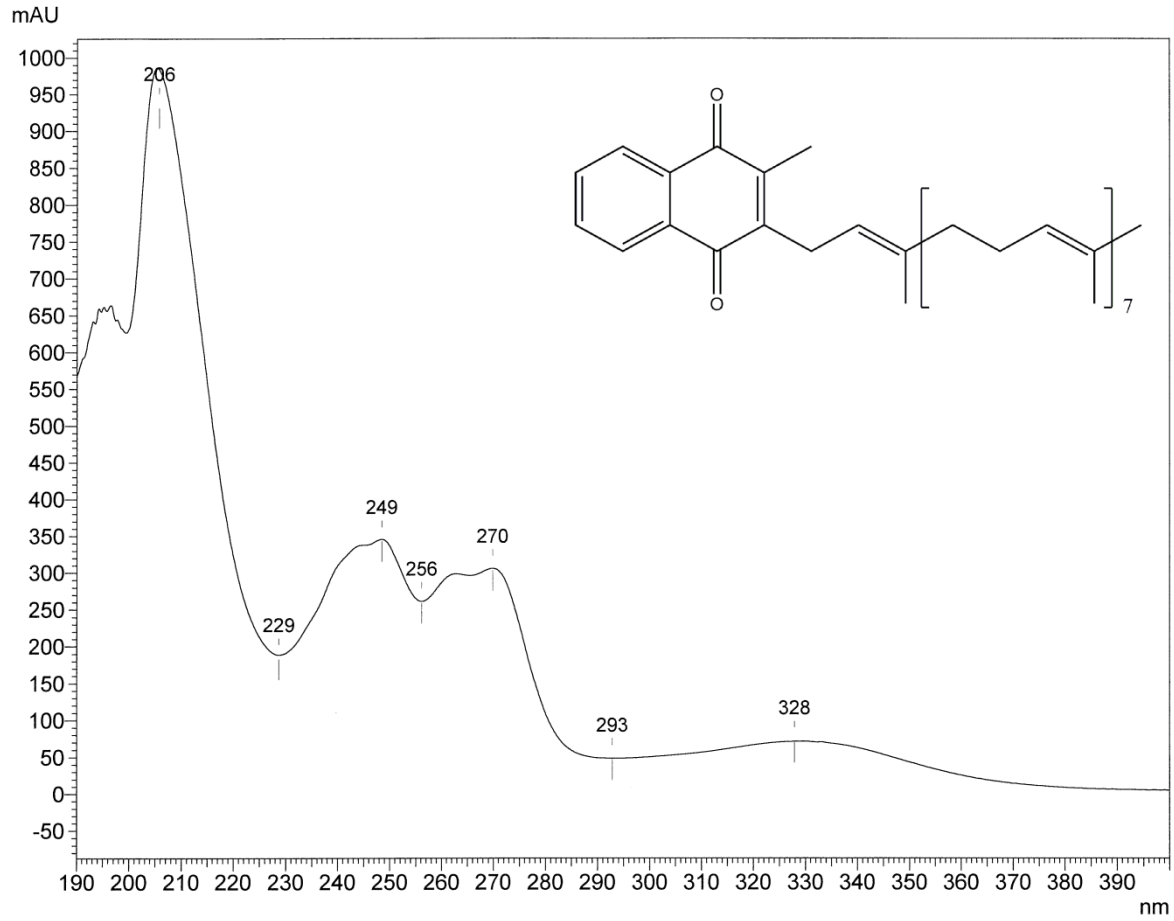

Figure S6. LCMS On-line UV-visible absorption spectrum of the peak representing MK-8 and the structure of MK-8.

REFERENCES

Aziz, R.K., Bartels, D., Best, A.A., DeJongh, M., Disz, T., Edwards, R.A., Formsma, K., Gerdes, S., Glass, E.M., Kubal, M., Meyer, F., Olsen, G.J., Olson, R., Osterman, A.L., Overbeek, R.A., McNeil, L.K., Paarmann, D., Paczian, T., Parrello, B., Pusch, G.D., Reich, C., Stevens, R., Vassieva, O., Vonstein, V., Wilke, A., and Zagnitko O. (2008). The RAST Server: Rapid annotations using subsystems technology. *BMC Genomics* **8,** 9:75.

Bligh, E. G. & Dyer, W. J. (1959). A rapid method of total lipid extraction and purification. *Can J Biochem Physiol* **37**, 911-917.

Carreau, J. P. & Dubacq, J. P. (1978). Adaptation of a macro scale method to the micro scale for fatty acid methyl transesterification of biological lipid extracts. *J Chromatogr* **151**, 384-390.

Desvaux, M., Hébraud, M., Talon, R., and Henderson, I.R. (2009). Secretion and subcellular localizations of bacterial proteins: a semantic awareness issue. *Trends Microbiol* **17:** 139–145.

Hardy, K. R. & King, G. M. (2001). Enrichment of high-affinity CO oxidizers in maine forest soil. *Appl Environ Microbiol* **67**, 3671-3676.

King, G. M. (2003). Molecular and culture-based analyses of aerobic carbon monoxide oxidizer diversity. *Appl Environ Microbiol* **69**, 7257-7265.

MacKenzie, A., Vyssotski, M. & Nekrasov, E. (2009). Quantative analysis of dairy phospholipids by ^{31}P NMR. *J Am Oil Chem Soc* **86**, 757-763.

Nishijima, A., Araki-Sakai, M., Sano, H. (1997). Identification of isoprenoid quinones by frit-FAB liquid chromatography–mass spectrometry for the chemotaxonomy of microorganisms. *J Microbiol Meth* **28**, 113-122.

Ramaley, R. F. & Hixson, J. (1970). Isolation of a nonpigmented, thermophilic bacterium similar to *Thermus aquaticus*. *J Bacteriol* **103**, 526-528.

Sherman, P. A. & Sander, E. G. (1981). Vitamin K epoxide reductase: Evidence that Vitamin K dihydroquinone is a product of Vitamin K epoxide reduction. *Biochem Biophys Res Commun* **103,** 997-1005.

Stránský, K., Jursík, T., Vítek, A. & Skořepa, J. (1992). An improved method of characterizing fatty acids by equivalent chain length values. *J High Res Chromatog* **15**, 730-740.

Suhara, Y., Wada, A., Tachibana. Y., Watanabe M., Nakamura, K., Nakagawa, K., Okano, T. (2010). Structure–activity relationships in the conversion of vitamin K analogues into menaquinone-4. Substrates essential to the synthesis of menaquinone-4 in cultured human cell lines. *Bioorg Med Chem* **18,** 3116-3124.

Sutcliffe, I. C. (2011). Cell envelope architecture in the *Chloroflexi*: a shifting frontline in a phylogenetic turf war. *Environ Microbiol* **13**, 279-282.

Tindall, B. J. (1990). Lipid-composition of *Halobacterium lacusprofundi*. *FEMS Microbiol Lett* **66**, 199-202.

Vaskovsky, V. E., Kostetsky, E. Y. & Vasendin, I. M. (1975). A universal reagent for phospholipid analysis. *J Chromatogr* **114**, 129-141.